Food and Bioproducts Processing 145 (2024) 148–157

Contents lists available at ScienceDirect

Food and Bioproducts Processing

journal homepage: www.elsevier.com/locate/fbp

Lychee peel extract-based magnetic iron oxide nanoparticles: Sustainable synthesis, multifaceted antioxidant system, and prowess in eco-friendly food preservation

Johar Amin Ahmed Abdullah [a,*], Cesar André Andino Perdomo [b], Luis Arturo Hernández Núñez [b], Octavio Rivera-Flores [b], Marlon Sánchez-Barahona [b], Antonio Guerrero [a], Alberto Romero [c]

[a] Departamento de Ingeniería Química, Escuela Politécnica Superior, Universidad de Sevilla, Sevilla 41011, Spain
[b] Unidad de Gestión de Investigación Científica, Ingeniería Agroindustrial, Universidad Nacional Autónoma de Honduras Tecnológico Danlí, Danlí 13201, Honduras
[c] Departamento de Ingeniería Química, Facultad de Física, Universidad de Sevilla, Sevilla 41012, Spain

ARTICLE INFO

Keywords:
Lychee peel extract
Magnetic iron oxide nanoparticles
Green nanotechnology
Antioxidant properties
Sustainable food preservation

ABSTRACT

The quest for sustainable synthesis methods has led to the exploration of lychee peel extract (LCPEx) as an eco-friendly alternative in the field of nanomaterials. This groundbreaking study introduces the synthesis of lychee peel extract-based magnetic iron oxide nanoparticles (LCPEx-MIONPs) and delves into their diverse applications. The meticulous methodology involved a multistep process for lychee peel extraction, resulting in the creation of LCPEx. The subsequent synthesis of LCPEx-MIONPs, achieved by combining the extract with iron chloride as a precursor and sodium hydroxide as a pH adjustor (set to 7.5), yielded nanoparticles with nanoscale dimensions (8.7± 0.4 nm) and diverse morphologies (cubic, hexagonal, spherical). Comprehensive characterization techniques, including Fourier transform infrared spectroscopy (FTIR), X-ray diffraction (XRD), scanning electron microscopy (SEM), and transmission electron microscopy (TEM), unveiled the structural attributes of LCPEx-MIONPs. The LCPEx exhibited robust antioxidant activity against DPPH, reaching its maximum inhibitory within only 5 minutes in a simple disc diffusion. The multifaceted antioxidant system of LCPEx-MIONPs exhibited an IC_{50} value of 202.3 μg/mL, highlighting the synergistic effects of lychee phytochemicals and magnetic ions. Beyond antioxidant capabilities, LCPEx-MIONPs, when incorporated into banana-based food preservation films, demonstrated significant prowess in grape preservation. The controlled release properties led to a notable reduction in water loss (9.3% on day 3 and 19.7% on day 6) compared to control grapes without LCPEx-MIONPs incorporated (18.2% on day 3 and 34.8% on day 6). This study significantly contributes to green nanotechnology, food preservation, and the development of eco-friendly hydrogels and bioplastic films, emphasizing the versatile applications of LCPEx-MIONPs in antioxidants, sustainable food preservation, and hydrogel-based bioplastics.

1. Introduction

Embarking on the intricate journey through nanomaterials demands a delicate balance between challenges and opportunities, propelling the scientific community towards innovative solutions (Fryxell and Cao, 2012). The conventional avenues of nanomaterial synthesis have long grappled with environmental concerns, prompting a resolute shift towards sustainable and green methodologies (Drummer et al., 2021). This transformation not only addresses ecological issues but also propels the field into a new era of responsible material science (Rane et al., 2018). Amidst the array of green methodologies, those harnessing the power of plant extracts emerge as beacons of sustainability (Patete et al., 2011). Particularly, lychee (Litchi chinensis) peel extract (LCPEx) stands out, offering a remarkable and eco-friendly approach to nanomaterial synthesis (Ramananda Singh et al., 2019). This plant-based exploration aligns not only with environmental consciousness but also demonstrates

* Corresponding author.
E-mail addresses: jabdullah@us.es (J.A.A. Abdullah), caandino@unah.hn (C.A.A. Perdomo), jorivera@unah.edu.hn (O. Rivera-Flores), marlon.sanchez@unah.edu.hn (M. Sánchez-Barahona), aguerrero@us.es (A. Guerrero), alromero@us.es (A. Romero).

https://doi.org/10.1016/j.fbp.2024.03.007
Received 6 February 2024; Received in revised form 14 March 2024; Accepted 29 March 2024
Available online 2 April 2024

potential applications in diverse areas of nanotechnology (Marslin et al., ; Tsao, 2010).

In this dynamic landscape, magnetic iron oxide nanoparticles have ascended to a prominent position, showcasing unique properties that set them apart from other materials (Marciello et al., 2013; Shah et al., 2019). Magnetic iron-based nanoparticles exhibit remarkable efficacy in environmental remediation, providing solutions such as water purification, soil revitalization, and toxic waste treatment. Their magnetic properties enable easy recovery, minimizing environmental impact. Current research focuses on refining designs for sustainable applications (Alangari et al., 2022; Herranz et al., 2008). Various methods, including inert gas condensation, high-energy ball milling, liquid-phase reduction, and reverse micelle, are widely employed for iron-based nanoparticle preparation (Darroudi et al., 2014; Marciniak et al., 2020). However, these methods, though effective, presents challenges due to chemical consumption, cost, and the generation of toxic by-products, potentially harmful to the environment (Maldonado-Camargo et al., 2017). Recent studies underscore the limitations of iron-based NPs, such as aggregation and oxidation. In response, green synthesis, utilizing plant extracts rich in non-toxic compounds like polyphenols and caffeine, emerges as an eco-friendly alternative (Chaudhuri and Malodia, 2017; Patiño-Ruiz et al., 2021).

The synthesis of metal nanoparticles holds significant importance due to their catalytic, optical, and electrical properties. Predominantly, chemical methods involve expensive and toxic reagents, potentially leading to environmental contamination (Qiao et al., 2017; Hangxun et al., 2013). Hence, there is a growing need in nanotechnology to develop green and environmentally friendly approaches for nanoparticle synthesis. Nanoparticle biosynthesis, particularly through biological methods using microorganisms or plant extracts, has gained prominence as an eco-friendly and benign alternative. In plant-mediated methods, the reaction time is significantly reduced compared to microorganism-mediated methods, ensuring efficiency in nanoparticle synthesis (Gour and Jain, 2019).

Highlighting the lychee (Litchi chinensis) peel extract (LCPEx) as a standout contributor, this study delves into its remarkable and eco-friendly approach to nanomaterial synthesis (Ramananda Singh et al., 2019). The rich phytochemical composition of lychee, encompassing flavonoids, carotenoids, and polyphenols, underlines its antioxidant capabilities. Lychee extracts, derived from this vibrant fruit, are increasingly recognized for their role in green synthesis processes (Ramananda Singh et al., 2019; Cefali et al., 2015). Laden with bioactive compounds, these extracts serve as eco-friendly and sustainable precursors for various nanoparticles (Shahzad et al., 2014). The amalgamation of lychee extracts with specific metallic ions facilitates the fabrication of diverse nanoparticle structures, including magnetic iron oxide nanoparticles (MIONPs) (Majeed et al., 2016). The inherent antioxidant properties of lychee, coupled with its compatibility in nanoparticle synthesis, open avenues for innovative applications—from biomedical fields to eco-friendly packaging solutions. As researchers delve deeper into harnessing the potential of plants, particularly lychee, in nanotechnology, the intrinsic qualities of this humble fruit continue to inspire novel advancements (Fahmy et al., 2018).

In the broader context of innovation, bioplastics, derived from renewable and/or biodegradable resources, are gaining momentum in the chemical and plastics industry (Cruz et al., 2022). Beyond the agri-food sector, they present new markets and business prospects. While various plastic-based bioresources like gelatin, chitosan, and cellulose acetate have been extensively studied, plant-based resources like banana-based bioplastics remain relatively limited (Cartwright et al., 2020).

This study introduces an innovative method for synthesizing lycee extract-magnetic iron oxide nanoparticles (LCPEx-MIONPs). It focuses on antioxidant capacity and food preservation in conjunction with banana-based bioplastics. The research aims to fully recycle lychee, converting its peels into useful nanomaterials and banana fruit waste into powder for bioplastic development, reducing agrowaste and promoting environmental conservation. Contributing to the expanding field of nanotechnology, the study provides valuable insights into the synthesis and versatile applications of LCPEx-MIONPs, inspiring further exploration in green chemistry and bioplastic development. The study's validation utilized advanced techniques, including X-ray diffraction, transmission electron microscopy, scanning electron microscopy, and Fourier transform infrared spectroscopy, to discern the distinct characteristics of magnetite structure and various morphologies. The investigation enhances our comprehension of novel nanocomposites, promising exciting possibilities for sustainable food preservation and packaging applications.

2. Materials and methods

2.1. Materials

The key reagents used were ethanol, 98% iron (III) chloride hexahydrate, sodium hydroxide, and 2,2-diphenyl-1-picrylhydrazyl (DPPH). All other chemicals were of analytical grade.

Lychee fruit was obtained locally, and banana powder for bioplastics was provided by the Bio-plastic Innovation Plant at the National Autonomous University of Honduras ((Castro-Criado et al., 2023) for details).

2.2. Lychee peel extract (LCPEx) preparation

Upon receiving lychee fruit, the peel extraction (LCPEx) process was initiated. After washing and disinfection, the peel was separated, chopped, and dried in trays at 90 °C for a total of 18 interrupted hours (14 hours drying, 2 hours without, and 4 hours drying). Subsequently, the dried peels underwent pulverization, sieving, and maceration. A concentrated solution was prepared by mixing 13 g of peel flour with 100 mL of distilled water, left to rest for 24 hours. Following this, the LCPEx underwent filtration using coffee paper, and the resulting extract was stored for antioxidant testing and nanoparticle preparation (Abdullah et al., 2022).

2.3. Nanoparticle fabrication

The LCPEx, obtained earlier, formed the basis for the synthesis of LCPEx-magnetic iron oxide nanoparticles (LCPEx-MIONPs). In a concise procedure, 50 mL of the acquired extract was blended with 1 M $FeCl_3\cdot 6H_2O$, and the pH was adjusted to 7.5 using 5 M NaOH (Abdullah et al., 2023a, 2023a). The solution underwent a discernible color change, signifying the precipitation of nanoparticles. Following this, the mixture underwent filtration and was subjected to a 24-hour drying process at 200 °C in an induction oven.

2.4. Nanoparticle characterization

2.4.1. Fourier transform infrared spectroscopy (FTIR)

To elucidate the structural details of LCPEx-MIONPs, Fourier Transform Infrared Spectroscopy (FTIR) was utilized, probing vibration modes within the range of 4000–400 cm^{-1}. Identification of Fe–O bonds in the MIO-NPs was achieved, particularly in the fingerprint region (800–400 cm^{-1}) (Abdullah et al., 2020).

2.4.2. X-ray diffraction (XRD)

X-ray Diffraction (XRD) patterns, acquired using a Bruker D8 Advance A25 diffractometer with Cu anode, were analyzed to affirm the crystalline phase, crystal systems, and to determine the size and degree of crystallinity of the LCPEx-MIONPs, following procedures outlined in a prior study (Abdullah et al., 2020). The diffractograms were recorded within the range of $2\theta = [15–70°]$.

2.4.3. Scanning electron microscopy (SEM)

The morphological and size attributes of the nanoparticles were discerned through Scanning Electron Microscopy (SEM) analysis. The investigation was conducted using a Zeiss EVO scanning electron microscope.

2.4.4. Transmission electron microscopy (TEM)

Transmission Electron Microscopy (TEM) analysis, utilizing a Talos S200 microscope (FEI, USA) operating at 200 kV, was carried out to ascertain the morphology and size of the nanoparticles.

2.5. Antioxidant activity of the LCPEx and LCPEx-MIONPs assessment

In the process of preparing LCPEx for iron oxide synthesis, we evaluated its antioxidant activity using Disc Diffusion against the DPPH free radical (Abdullah et al., 2023a). To assess antioxidant activity, 25 mL of an oxidizing solution (DPPH 7 mg/100 mL in ethanol) was placed in a Petri dish. Then, 1 mL of concentrated LCPEx was added. The DPPH solution (7 mg in 100 mL ethanol) was cast onto a 10 cm diameter aluminum plate, and 1 mL of LCPEx was applied to the center. The color changed immediately to clear yellow. Antioxidant activity was assessed by measuring color change areas using ImageJ software.

The employed assessment method has been validated by quantifying the area, and the inhibition percentage was calculated using the following equation:

$$\text{Inhibition}(\%) = \left(\frac{A_1 - A_2}{A_1}\right) \times 100 \quad (1)$$

In this equation, A1 represents the total area of the inhibited DPPH with purple color, and A2 represents the remaining areas without a change in color over time. A complete color change to yellow is recorded as 100% inhibition. This method serves as a valuable tool for quantifying the antioxidant capacity of the plant extract, particularly LCPEx, offering crucial insights into its potential applications, including the synthesis of iron oxide nanoparticles. For LCPEx-MIONPs, the antioxidant activity was assessed using the protocol outlined in (Hangxun et al., 2013).

2.6. Grape preservation

Grapes, being nutrient-rich yet vulnerable to microbial deterioration, were chosen as the subject for evaluating the viability of utilizing LCPEx-MIONPs stabilized with banana-based bioplastic as a bio-coating and material for food nanopackaging. To treat the grapes, an aqueous solution of banana water (1:3 ratio) was prepared, involving the dissolution of 1 g in 30 mL of water. The mixture underwent stirring for approximately 10 minutes at 100 °C. Following this, the solution was filtered using coffee filtration paper, and the resultant liquid, constituting the banana-based bioplastic, was collected. Subsequently, about 7 mg of LCPEx-MIONPs were introduced and manually mixed into the banana solution. In the final step, the grapes were immersed in the resulting solution for a duration of 3 minutes and left for a 6-day shelf-life test at room temperature (28±7 °C and an average relative humidity (RH) of 87%).

At three-day intervals, images were captured, and the weight loss rate (WLR, %) was computed using the formula:

$$\text{WLR}(\%) = \left(\frac{P_{Fresh} - P}{P_{Fresh}}\right) \times 100 \quad (2)$$

In this equation, P_{Fresh} and P denote the weights of fresh and preserved grapes, respectively (Mohammed et al., 2023).

3. Results

3.1. FTIR

The lychee (Lichi chinesis) peel extract-based magnetic iron oxide nanoparticles (LCPEx-MIONPs) underwent characterization through Fourier Transform Infrared Spectroscopy (FTIR) to elucidate the functional groups present in the samples (Fig. 1). Analysis of the FTIR spectra revealed distinctive peaks at various wavenumbers: 3364.64, 2957.47, 2060.87, 1675.39, 1429.13, 1063.81, 924.07, 864.65, 687.62, 564.25, and 432.21 cm^{-1}.

The prominent peak at 3364.64 cm^{-1} is indicative of the presence of O-H stretching vibrations, suggesting the involvement of hydroxyl groups (Rajeswari et al., 2021). The peaks observed at 2957.47 cm^{-1} corresponds to –CH_2 and C-H stretching vibrations in aliphatic compounds (Wang et al., 2014). The wavenumbers 2060.87 cm^{-1} are associated with the presence of C=O stretching vibrations (Chandrasekar et al., 2013).

The peak at 1675.39 cm^{-1} can be attributed to -OH, C=C, and C=O groups (Aksu Demirezen et al., 2019; Huang et al., 2014; Abdullah et al., 2017), as shown in Fig. 1(a). Additionally, the peaks at 1429.13 cm^{-1}, 1063.81 cm^{-1}, 924.07, and 864.65 cm^{-1} are indicative of C-H bending vibrations in alkanes, C-O stretching vibrations in ethers, and C-O stretching vibrations in alcohols, respectively (Salgado et al., 2019a; Guerrero-Pérez and Patience, 2020).

Furthermore, the peaks in the range of 900–400 cm^{-1} may be associated with Fe-O stretching vibrations, signifying the presence of iron oxide in the nanoparticle structure (Wang et al., 2014; Manzo et al., 2020; Tadic et al., 2019). Specifically, these peaks were identified at 687.62, 564.25, and 432.21 cm^{-1}, as shown in Fig. 1(b).

The FTIR analysis of LCPEx-MIONPs revealed a diverse array of functional groups, including hydroxyl, aliphatic, nitrile, isocyanate, amine, alkane, ether, alcohol, and metal oxide groups. These findings provide valuable insights into the chemical composition of the synthesized magnetic iron oxide nanoparticles, underscoring the versatility and complexity of the lychee peel extract-based nanomaterial.

3.2. XRD

The magnetic iron oxide nanoparticles derived from lychee peel extract (LCPEx-MIONPs) underwent comprehensive evaluation through X-ray diffraction (XRD), as depicted in Fig. 2(a). Additionally, a visual representation of the magnetic response to the magnet is presented in Fig. 2(b).

The XRD analysis unveiled peaks at 2θ values (hkl), corresponding to crystallographic planes, including peaks at 30.17° (220), 31.76 (202), 35.43° (311), 43.14° (400), 48.31° (331), 62.65° (440), and 66.31° (531) were identified, corresponding to cubic magnetite with space group F d −3 m:2 (227), as per JCPDS card number 00–900–2317 (53.8%) (Haavik et al., 2000). Additionally, peaks at 49.75° (300) and 56.74° (009) were attributed to the trigonal structure of magnetite, space group R −3 m:H (166), in accordance with JCPDS card number 00–152–6955 (15.4%) (Wright et al., 2000). Further peaks at 24.06° (112), 27.44° (113), 40.02° (116), and 45.49° (030) were ascribed to monoclinic magnetite with space group P 12/c 1 (13), according to JCPDS card number 00–153–2800 (30.8%) (Wright et al., 2002). The XRD analysis underscored the diverse crystal systems within LCPEx-MIONPs, each with varying percentages. Fig. 3 illustrates the distinct crystal systems identified through XRD.

Interestingly, a study by Abdullah et al (Abdullah et al., 2023a, 2023b). demonstrated that the coexistence of both cubic and monoclinic systems enhances the magnetic response, aligning with our observations in Fig. 2(b). The presence of the trigonal system was noted to influence their response, potentially explaining the partial response of these particles to the magnet due to interactions between different crystal structures. Furthermore, the assessment of crystallite size indicated an

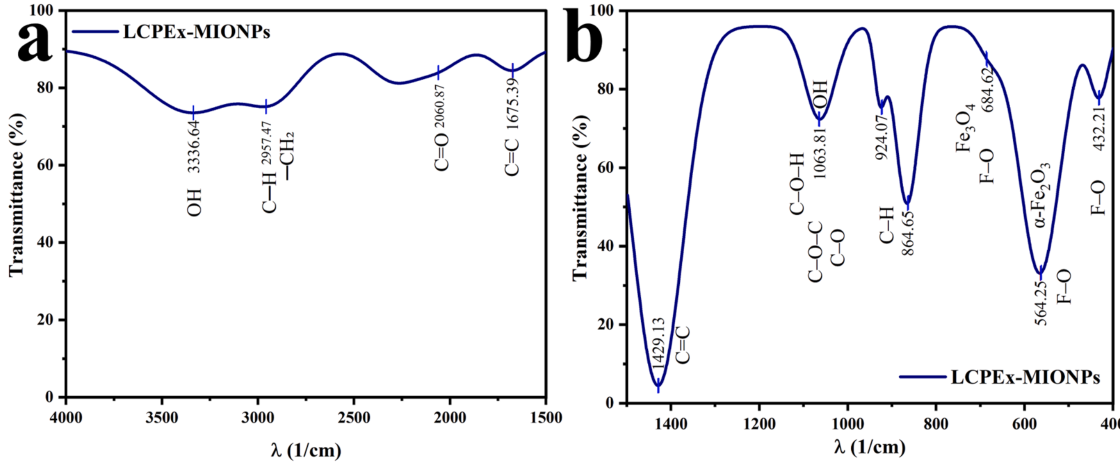

Fig. 1. FTIR spectra of lychee peel extract-based magnetic iron oxide nanoparticles (LCPEx-MIONPs), illustrating characteristic peaks corresponding to various functional groups within the chemical composition. (a) Shows the spectrum in the range of 4000–1500 cm^{-1}, while (b) presents the spectrum in the range of 1500–400 cm^{-1}.

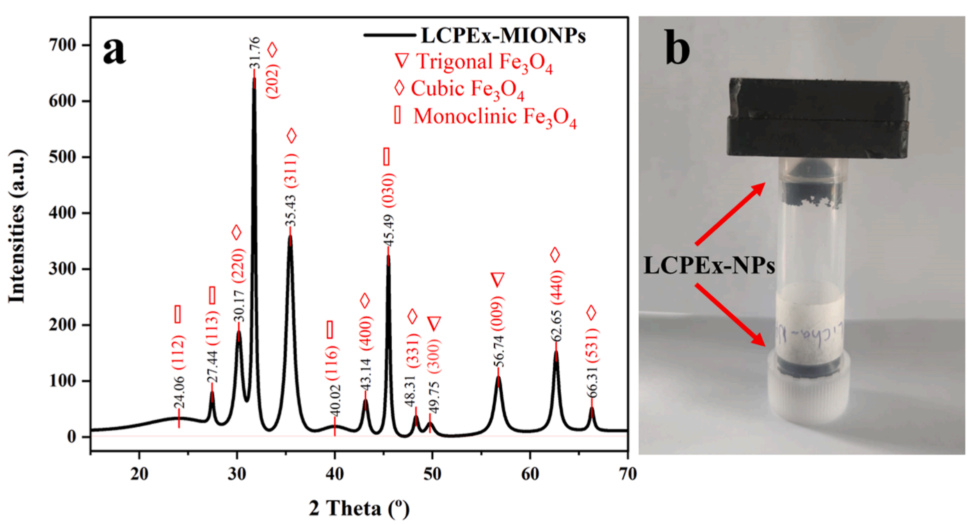

Fig. 2. : XRD results for LCPEx-MIONPs, illustrating crystallographic peaks characteristic of trigonal, cubic, and monoclinic Fe_3O_4 (a), complemented by visual magnetic responses of these structures (b).

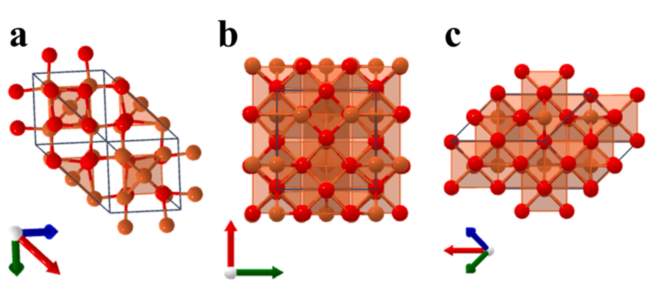

Fig. 3. : The model structure of the XRD analysis unveils the crystallographic behavior of LCPEx-MIONPs, highlighting distinct phases, such as (a) cubic, (b) monoclinic, and (c) trigonal Fe_3O_4.

average of 12.7 nm, validating the magnetic response as smaller nanoparticles exhibited a more pronounced reaction to the magnet (Vargas et al., 2007; Demortière et al., 2011). To further investigate, the morphology of LCPEx-MIONPs was analyzed using scanning electron microscopy (SEM) techniques and transmission electron microscopy (TEM).

3.3. SEM

Fig. 4 provides an insightful exploration of the complex particle assembly in the synthesized LCPEx-MIONPs, unveiling a dynamic interplay of diverse shapes and structures. The SEM images exhibit a predominant spherical assembly, along with nanosheets, nanoplates, and slender nano-tubes or nanowires (Fig. 4.a). The nanoparticle assemblies in this study replicate collaborative dynamics where various particles intricately coalesce through a synergistic interplay of phytochemicals and magnetic ions, forming agglomerates and aggregates.

Careful processing of SEM images was conducted using ImageJ software's image calculator, involving thresholding and Gaussian blur filters. The analyzed LCPEx-MIONPs underwent Gauss fit analysis with OriginLab, revealing an assembled nanoparticle diameter of 191.6 ± 52 nm, as depicted in Fig. 4.b (Abdullah et al., 2023b). Furthermore, the diameter distribution of nanoparticles, ranging from 11 to 39 nm, shows an average diameter of 13.9 ± 3.2 nm in Fig. 4.c, aligning with XRD measurements. The observed difference in nanoparticle size (191.6 ± 52) from SEM analysis, compared to XRD and TEM measurements, can be attributed to inherent disparities in these characterization techniques. XRD primarily reveals crystallographic information, while TEM

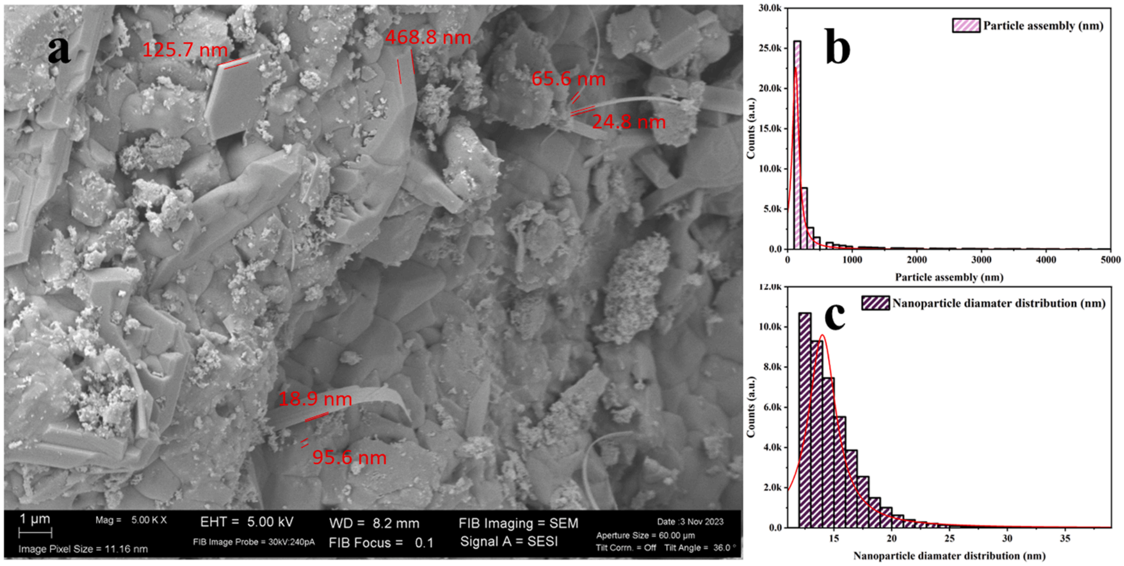

Fig. 4. **:** SEM images of LCPEx-MIONPs (a). The size distribution of particle assembly (agglomerate), ranging from 0 to 5000 nm, has an average size of 191.6 ± 52 nm (b). The diameter distribution of nanoparticles, ranging from 11 to 39 nm, has an average diameter of 13.9 ± 3.2 nm (c).

provides detailed views of individual particles. SEM, capturing a broader assembly, incorporates the collective dimensions of agglomerates and aggregates. These variations arise from the distinct methodologies of each technique, emphasizing the need for a comprehensive understanding through the integration of data from diverse characterization approaches (Tuoriniemi et al., 2014). Analogous morphologies have been documented in prior studies, as evidenced by research findings presented in references (Venkateswarlu et al., 2014; Avolio et al., 2019).

The distinct morphological assembly showcased in Fig. 4.a not only accentuates the innovative synthesis method but also underscores the broad spectrum of potential applications for LCPEx-MIONPs. The amalgamation of distinctive shapes, varied sizes, and magnetic properties enhances their versatility, making them well-suited for a range of applications, spanning from biomedical uses to environmental remediation (Fahmy et al., 2018). The intricate particle assembly portrayed in the images significantly contributes to our comprehensive comprehension of the synthesized nanoparticles, emphasizing their potential as multifunctional materials with diverse and impactful applications in various fields.

3.4. TEM

Fig. 5 presents the TEM analysis of LCPEx-MIONPs, unveiling a varied range of morphologies encompassing cubic, hexagonal, and spherical nanoparticles. In Fig. 5.a, discernible cubic nanoparticles, ranging from 2 to 23 nm, exhibit an average diameter distribution of 8.7 ± 0.4 nm, as depicted in Fig. 4.b. The distinctive features of these nanoparticles, characterized by their compact form and magnetic properties, underscore their promising potential for applications in medicine, electronics, and nanotechnology (Avolio et al., 2019; Park et al., 2018).

It is essential to emphasize that the size and shape of nanoparticles significantly impact their properties and behavior. The average diameter serves as a crucial metric for characterizing nanoparticle size, while the assessment of size distribution is equally vital. This distribution can vary, encompassing highly uniform nanoparticles to those with more dispersed sizes.

3.5. Antioxidant activity

The antioxidant activity assessment of LCPEx using the DPPH free radical assay yielded compelling results, highlighting the rapid and efficient nature of its antioxidant capabilities. The progressive increase in inhibition percentages, from 12.4% at 1 second to an impressive 100% at 5 minutes, suggests a swift and potent reaction against the DPPH radicals, as shown in Fig. 6.

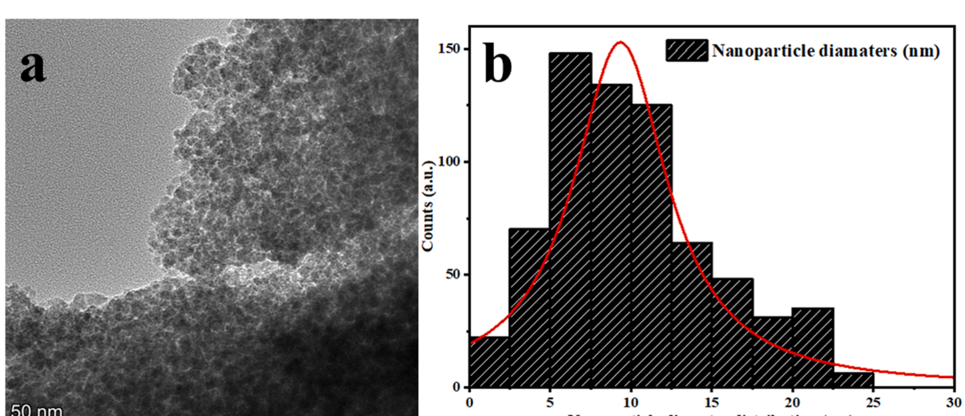

Fig. 5. TEM analysis of LCPEx-MIONPs displays diverse morphologies, including cubic nanoparticles (a) with their average diameter distribution (b).

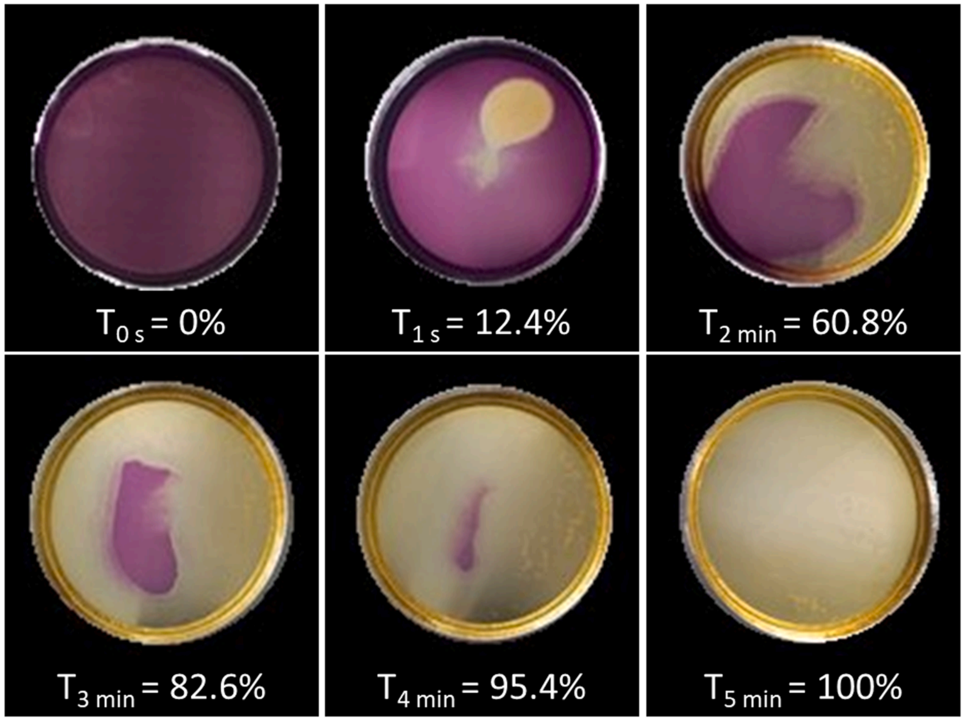

Fig. 6. Assessment of LCPEx antioxidant activity against DPPH free radicals across varied time intervals, supported by visualized photographs illustrating color transformations from dark purple to clear yellow.

This remarkable efficacy is indicative of the presence of powerful antioxidant compounds within LCPEx. The achievement of 100% inhibition within just 5 minutes is particularly noteworthy. This high inhibition percentage, coupled with the complete color change from purple to clear yellow, underscores the thoroughness of LCPEx in neutralizing DPPH radicals. The robust inhibitory effect implies a substantial concentration of bioactive compounds capable of effectively scavenging free radicals, positioning LCPEx as a promising candidate for antioxidant applications (Cefali et al., 2015; Salgado et al., 2019a; Islam et al., 2023). Beyond its antioxidant properties, the implications of these results extend to the synthesis of iron oxide nanoparticles (LCPEx-MIONPs). The swift and efficient reduction of DPPH radicals by LCPEx suggests its potential utility as a potent reducing agent in the green synthesis of nanoparticles. The rapid antioxidant response may play a crucial role in influencing the controlled synthesis of iron oxide nanoparticles, potentially impacting their size and morphology. While the DPPH assay provides valuable insights, it is essential to acknowledge its limitations, such as its focus on a single type of radical. A comprehensive understanding of LCPEx's antioxidant profile would benefit from the inclusion of complementary assays targeting different reactive species. Comparisons with other antioxidant assays could provide a more nuanced perspective on the overall antioxidant capacity of LCPEx.

Furthermore, it is important to recognize the preliminary nature of these findings and consider them as a basis for future investigations. Additional studies involving diverse antioxidant assays and the identification of specific bioactive compounds in LCPEx would enhance our understanding of its antioxidant potential. Exploring the kinetics of the antioxidant reaction could shed light on the underlying mechanisms driving the observed rapid inhibition. The results of the DPPH assay underscore the potent antioxidant activity of LCPEx, achieving 100% inhibition within 5 minutes. This rapid and efficient response holds promise for various applications, particularly in the synthesis of iron oxide nanoparticles. The findings contribute valuable insights into the biological activities of LCPEx and its potential role in the emerging field of nanomaterial synthesis.

Following the successful synthesis of LCPEx-MIONPs utilizing the highly bioactive antioxidant agent, the resulting nanoparticles were subjected to evaluation against DPPH free radicals, this time in concentration-dependent assays. The obtained data, represented in Fig. 7, showcased an IC_{50} value of 202.3 μg/mL for LCPEx-MIONPs. This finding emphasizes the considerable antioxidant potential inherent in these magnetic nanoparticles.

The observed high antioxidant activity of LCPEx-MIONPs can be attributed to the synergistic effects arising from the distinctive combination of lychee phytochemicals present in LCPEx and the structural attributes of the magnetic ions (Apak et al., 2007; Kanagasubbulakshmi and Kadirvelu, 2017). The incorporation of bioactive compounds from the lychee extract contributes significantly to the overall antioxidant capacity of the nanoparticles. Simultaneously, the magnetic ions in the

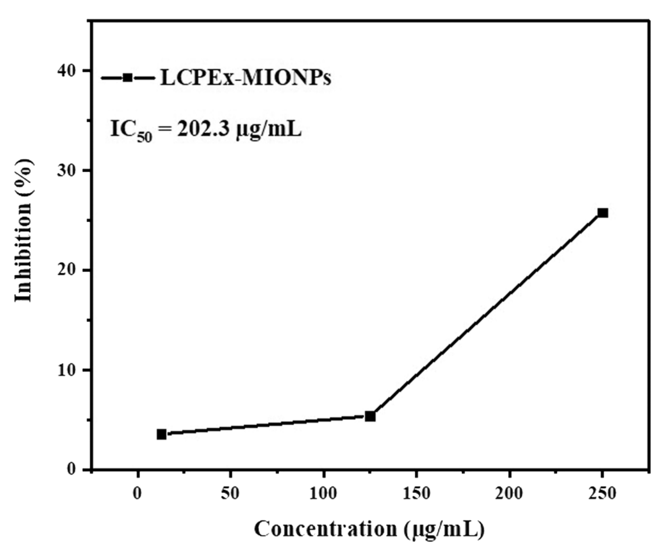

Fig. 7. Evaluation of Antioxidant Activity in LCPEx-MIONPs, Highlighting an IC_{50} Value of 202.3 μg/mL.

nanoparticle structure may play a crucial role in enhancing the scavenging capabilities against free radicals.

This dual contribution from both the plant-derived antioxidants and the magnetic nanoparticle structure highlights the potential of LCPEx-MIONPs as a multifunctional material. Beyond their role in antioxidant applications, these nanoparticles may find utility in various fields, including biomedical and environmental sectors, where their magnetic properties could be leveraged for targeted drug delivery or pollutant removal. The results presented underscore the versatility and promise of LCPEx-MIONPs as a novel and potent antioxidant nanomaterial.

The determined size of LCPEx-MIONPs, as assessed through TEM with measurements of 8.7± 0.4 nm and XRD revealing 12.7 nm, emerges as a pivotal determinant for their heightened antioxidant efficacy. The nanoscale dimensions of these nanoparticles play a critical role in amplifying their surface area, facilitating enhanced interactions with free radicals, thereby bolstering their scavenging capabilities (Shah et al., 2019; Affes et al., 2020; Zhao et al., 2018). This phenomenon gains further credence from the diverse shapes captured in TEM images, illustrating ultrasmall cubic, hexagonal, and spherical forms, each measuring less than 20 nm. This variety in morphologies signifies a heterogeneous distribution of particle shapes, potentially leading to varied reactivity towards free radicals (Rajakumar et al., 2018). Furthermore, the inclusion of magnetic ions within the nanoparticle structure significantly contributes to their antioxidant activity (Santoyo Salazar et al., 2011). The inherent magnetic properties in LCPEx-MIONPs may facilitate electron transfer reactions, actively participating in the reduction of free radicals and subsequently enhancing their antioxidant efficacy. This unique characteristic adds an additional dimension to their antioxidant activity, setting them apart from conventional antioxidant agents.

The concurrent presence of lychee phytochemicals and magnetic ions establishes a multifaceted antioxidant system within LCPEx-MIONPs, where these various components synergistically collaborate to efficiently neutralize free radicals (Cartwright et al., 2020). Mechanisms for phytochemicals and magnetite (Fe_3O_4) nanoparticles' antioxidant activity, involving processes such as single-electron transfer (SET) and hydrogen atom transfer (HAT) (Abdullah et al., 2023a), are illustrated in Fig. 8.

In SET, the formation of the energetically stable species DPPH– occurs, resulting in the antioxidant cation radical ($R\text{-}OH^{+\bullet}$) with stabilized

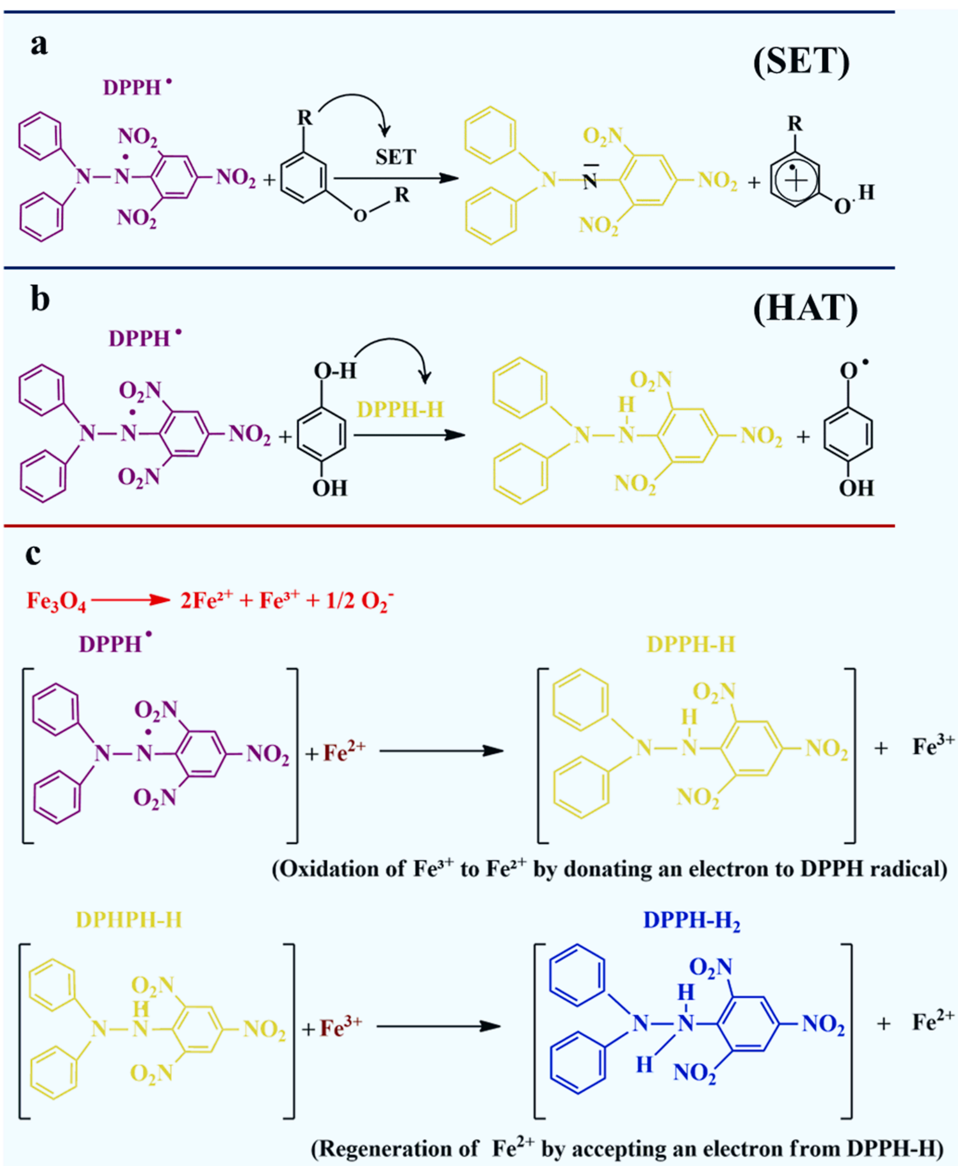

Fig. 8. Proposed mechanisms for the antioxidant activity of phytochemicals and magnetite (Fe_3O_4) nanoparticles, including (a) SET mechanism, (b) HAT mechanism, and (c) SET mechanism specifically for magnetite (Fe_3O_4) antioxidants.

odd electrons (Leopoldini et al., 2011). This is illustrated in Fig. 8(a). In HAT, antioxidants donate a hydrogen atom to free radicals, forming a stabilized neutral species while turning into an antioxidant free radical (Zeb, 2020), as shown in Fig. 8(b). The antioxidant function of polyphenolic compounds, such as gallic acid in lychee peel extract, relies on the benzene ring and hydroxyl group arrangement. The stability of antioxidant molecules during interactions with free radicals is significantly influenced by the presence of the benzene ring (Phenols et al., 2006). Lychee peel extract, rich in phenolic compounds, efficiently neutralizes DPPH within a short period (5 min), shifting its color from purple to yellow.

Concerning the neutralization of DPPH free radicals by iron oxide antioxidants like Fe_3O_4, the transfer of electrons neutralizes the radical due to the redox properties of iron ions. In the case of Fe_3O_4, an oxide exhibiting mixed valence, the continuous reduction of DPPH is facilitated by the direct donation of electrons from Fe^{2^*} ions and the subsequent regeneration of Fe^{2+} through redox cycling by Fe^{3+} ions (Perron et al., 2010; Perron and Brumaghim, 2009). This process is illustrated in Fig. 8(c). The specific mechanisms are influenced by various factors, encompassing crystal structure, particle size, surface area, magnetic behavior, DPPH preparation, and other experimental conditions (Affes et al., 2020; Rajakumar et al., 2018). The detailed chemical mechanisms depicted in Fig. 8(c) elucidate the oxidation of Fe_3O_4, the generation of Fe^{3+} ions, electron transfer to the DPPH radical, and the subsequent formation of a stable DPPH-H species. These mechanisms may encompass multiple steps and intermediates. Furthermore, the magnetic iron oxide nanoparticles provide convenient reusability through easy recovery using a magnet, maintaining their antioxidant capacity over multiple cycles and suggesting a potential for extended shelf life.

This innovative amalgamation of natural plant-derived compounds and magnetic nanoparticles not only enhances antioxidant capabilities but also holds promise for diverse applications, including the biomedical and environmental fields. The demonstrated versatility in shape, size, and structural attributes, as revealed by TEM and XRD analyses, collectively contributes to the superior antioxidant performance of LCPEx-MIONPs, positioning them as promising candidates for further exploration in both nanotechnology and antioxidant applications.

3.6. Grape preservation

In the realm of fruit preservation, the combination of LCPEx-MIONPs with bioplastic has been specifically evaluated using grapes as the selected fruit. In the control group devoid of LCPEx-MIONPs, a notable decrease in water content was observed, with an 18.2% loss by day 3 and a substantial 34.8% reduction by day 6 (refer to Fig. 9). In marked contrast, grape samples subjected to preservation with LCPEx-MIONPs, derived from lychee peel extract-based magnetic iron oxide nanoparticles, exhibited a remarkable preservation efficacy. These samples demonstrated only a 9.3% water loss on day 3 and a comparatively lower 19.7% loss on day 6. These findings unequivocally illustrate the superior preservation capacity of LCPEx-MIONPs nanoparticles in the context of food preservation, thereby underscoring their potential as a valuable and environmentally friendly solution for prolonging the shelf life of perishable produce. The substantial reduction in water loss observed in grapes treated with LCPEx-MIONPs highlights the efficacy of this innovative preservation approach, offering promise for sustainable practices in food storage and contributing to the overarching goal of minimizing food wastage (Galus et al.,). The ability of LCPEx-MIONPs to control release properties and exert stabilizing effects plays a pivotal role in diminishing water loss and preserving the freshness of grapes over an extended period.

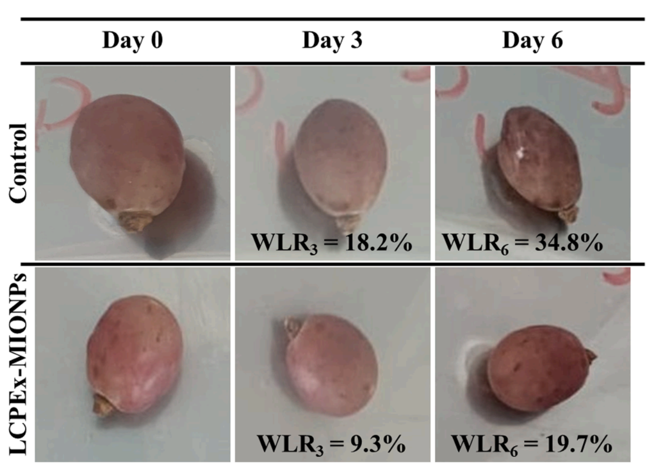

Fig. 9. Visual representation of photographs illustrating water content variation in grapes during preservation with LCPEx-MIONPs and the control without LCPEx-MIONPs. The values for water loss rate on days 3 and 6 of preservation are also provided.

4. Conclusions

The synthesis of lychee peel extract-based magnetic iron oxide nanoparticles (LCPEx-MIONPs) represents a significant advancement in the dynamic field of nanomaterials. This study successfully demonstrated the feasibility of utilizing lychee peel extract as a green alternative for the sustainable synthesis of magnetic nanoparticles with diverse morphologies and nanoscale dimensions. The comprehensive characterization using advanced techniques such as FTIR, XRD, SEM, and TEM provided valuable insights into the structural attributes of LCPEx-MIONPs. The multifaceted antioxidant system exhibited by LCPEx-MIONPs, with an IC_{50} value of 202.3 μg/mL, highlights the synergistic effects of lychee phytochemicals and magnetic ions. Beyond antioxidant capabilities, these nanoparticles demonstrated significant potential in grape preservation. The controlled release properties of LCPEx-MIONPs led to a notable reduction in water loss in grapes, emphasizing their efficacy in sustainable food preservation.

However, it is essential to acknowledge the limitations of this study, particularly in the laboratory setting. Future research should address these limitations to enhance the practical applicability of LCPEx-MIONPs. For instance, further studies could explore the scalability and reproducibility of the synthesis process to facilitate large-scale production. Additionally, in vivo studies are crucial to evaluate the safety and potential toxicity of these nanoparticles in living organisms. Moreover, future investigations could leverage more advanced techniques, such as advanced spectroscopy and imaging methods, to gain a deeper understanding of the interactions between LCPEx-MIONPs and biological systems. This could aid in optimizing the design of these nanoparticles for specific biomedical applications. In conclusion, this study opens new avenues in the field of green nanotechnology, showcasing LCPEx-MIONPs as versatile and eco-friendly materials with impactful applications in antioxidants and sustainable food preservation. Addressing laboratory limitations and advancing research through more sophisticated techniques and in vivo studies will undoubtedly contribute to the continued progress and broader adoption of these green nanomaterials in various fields.

Ethic approval

Not applicable.

Funding

This study was financially supported by MCIN/AEI/10.13039/501100011033 / FEDER, UE, through the project PID2021–124294OB-C21. International Cooperation Project Ref. 2022/ACDE/000265 funded by the Agencia Española de Cooperación Internacional (AECID).

Declaration of Competing Interest

The authors declare that they have no known competing financial interests or personal relationships that could have appeared to influence the work reported in this paper.

Acknowledgments

The authors acknowledge the MCI/AEI/FEDER, EU project (Ref. PID2021–124294OB-C21) that supports this work. In addition, the authors thank the CONVOCATORIA DE AYUDAS PARA LA FORMACIÓN EN COOPERACIÓN INTERNACIONAL PARA EL DESARROLLO CON ESTANCIAS EN TERRENO 2022/2023. J.A.A.A. would like to thank the support from the Hayel Saeed Anam Group represented by Abdul Jabbar Hayel Saeed Anam. The authors express gratitude to CITIUS for providing access to and assisting with the SEM and TEM area characterization under microscopy services. Additionally, the authors appreciate the support received from CITIUS for FTIR microanalysis services and XRD characterization area.

Consent for publication

This manuscript has been submitted with the consent of all authors for publication.

References

Fryxell, G.E., Cao, G., 2012. Environmental Applications of Nanomaterials. IMPERIAL COLLEGE PRESS. https://doi.org/10.1142/p814.

Drummer, S., Madzimbamuto, T., Chowdhury, M., 2021. Green synthesis of transition-metal nanoparticles and their oxides: a review. Mater. (Basel) 14, 2700. https://doi.org/10.3390/ma14112700.

Rane, A.V., Kanny, K., Abitha, V.K., Thomas, S., 2018. Methods for synthesis of nanoparticles and fabrication of nanocomposites. Synth. Inorg. Nanomater. Elsevier, pp. 121–139. https://doi.org/10.1016/B978-0-08-101975-7.00005-1.

Patete, J.M., Peng, X., Koenigsmann, C., Xu, Y., Karn, B., Wong, S.S., 2011. Viable methodologies for the synthesis of high-quality nanostructures. Green. Chem. 13, 482–519. https://doi.org/10.1039/c0gc00516a.

Ramananda Singh, M., Gupta, P., Gupta, K., 2019. The litchi (Litchi chinensis) peels extract as a potential green inhibitor in prevention of corrosion of mild steel in 0.5 M H2SO4 solution. Arab. J. Chem. 12, 1035–1041. https://doi.org/10.1016/j.arabjc.2015.01.002.

G. Marslin, K. Siram, Q. Maqbool, R. Kamalabai Selvakesavan, D. Kruszka, P. Kachlicki, G. Franklin, materials Secondary Metabolites in the Green Synthesis of Metallic Nanoparticles, (n.d.). https://doi.org/10.3390/ma11060940.

H.M. Fahmy, F.M. Mohamed, M.H. Marzouq, A.B.E. Mustafa, Review of Green Methods of Iron Nanoparticles Synthesis and Applications, (2018).

Tsao, R., 2010. Chemistry and biochemistry of dietary polyphenols. Nutrients 2, 1231–1246. https://doi.org/10.3390/nu2121231.

Marciello, M., Connord, V., Veintemillas-Verdaguer, S., Vergés, M.A., Carrey, J., Respaud, M., Serna, C.J., Morales, M.P., 2013. Large scale production of biocompatible magnetite nanocrystals with high saturation magnetization values through green aqueous synthesis. J. Mater. Chem. B. 1, 5995–6004. https://doi.org/10.1039/c3tb20949k.

Shah, S.T., Yehye, W.A., Chowdhury, Z.Z., Simarani, K., 2019. Magnetically directed antioxidant and antimicrobial agent: Synthesis and surface functionalization of magnetite with quercetin. PeerJ 2019, 1–22. https://doi.org/10.7717/peerj.7651.

Alangari, A., Alqahtani, M.S., Mateen, A., Kalam, M.A., Alshememry, A., Ali, R., Kazi, M., Alghamdi, K.M., Syed, R., 2022. Iron Oxide Nanoparticles: Preparation, Characterization, and Assessment of Antimicrobial and Anticancer Activity. Adsorpt. Sci. Technol. 2022 https://doi.org/10.1155/2022/1562051.

Aksu Demirezen, D., Yıldız, Y.Ş., Yılmaz, Ş., Demirezen Yılmaz, D., 2019. Green synthesis and characterization of iron oxide nanoparticles using Ficus carica (common fig) dried fruit extract. J. Biosci. Bioeng. 127, 241–245. https://doi.org/10.1016/j.jbiosc.2018.07.024.

Herranz, F., Morales, M.P., Roca, A.G., Vilar, R., Ruiz-Cabello, J., 2008. A new method for the aqueous functionalization of superparamagnetic Fe2O3 nanoparticles. Contrast Media Mol. Imaging 3, 215–222. https://doi.org/10.1002/cmmi.254.

Darroudi, M., Hakimi, M., Goodarzi, E., Kazemi Oskuee, R., 2014. Superparamagnetic iron oxide nanoparticles (SPIONs): Green preparation, characterization and their cytotoxicity effects. Ceram. Int. 40, 14641–14645. https://doi.org/10.1016/j.ceramint.2014.06.051.

Marciniak, L., Nowak, M., Trojanowska, A., Tylkowski, B., Jastrzab, R., 2020. The effect of ph on the size of silver nanoparticles obtained in the reduction reaction with citric and malic acids. Mater. (Basel) 13, 1–12. https://doi.org/10.3390/ma13235444.

Maldonado-Camargo, L., Unni, M., Rinaldi, C., 2017. Magnetic characterization of iron oxide nanoparticles for biomedical applications. Methods Mol. Biol. 1570, 47–71. https://doi.org/10.1007/978-1-4939-6840-4_4.

Chaudhuri, S.K., Malodia, L., 2017. Biosynthesis of zinc oxide nanoparticles using leaf extract of Calotropis gigantea: characterization and its evaluation on tree seedling growth in nursery stage. Appl. Nanosci. 7, 501–512. https://doi.org/10.1007/s13204-017-0586-7.

Patiño-Ruiz, D.A., Meramo-Hurtado, S.I., González-Delgado, Á.D., Herrera, A., 2021. Environmental Sustainability Evaluation of Iron Oxide Nanoparticles Synthesized via Green Synthesis and the Coprecipitation Method: A Comparative Life Cycle Assessment Study. ACS Omega 6, 12410–12423. https://doi.org/10.1021/acsomega.0c05246.

Qiao, S.Z., Liu, J., Max Lu, G.Q., 2017. Synthetic Chemistry of Nanomaterials. Elsevier B. V. https://doi.org/10.1016/B978-0-444-63591-4.00021-5.

Hangxun, X., Zeiger, B.W., Suslick, K.S., 2013. Sonochemical synthesis of nanomaterials. Chem. Soc. Rev. 42, 2555–2567. https://doi.org/10.1039/c2cs35282f.

Gour, A., Jain, N.K., 2019. Advances in green synthesis of nanoparticles. Artif. Cells, Nanomed. Biotechnol. 47, 844–851. https://doi.org/10.1080/21691401.2019.1577878.

Cefali, L.C., Cazedey, E.C.L., Souza-Moreira, T.M., Correa, M.A., Salgado, H.R.N., Isaac, V.L.B., 2015. Antioxidant activity and validation of quantification method for lycopene extracted from tomato. J. AOAC Int. 98, 1340–1345. https://doi.org/10.5740/jaoacint.14-151.

Shahzad, T., Ahmad, I., Choudhry, S., Saeed, M.K., Khan, M.N., 2014. Dpph free radical scavenging activity of tomato, cherry tomato and watermelon: Lycopene extraction, purification and quantification. Int. J. Pharm. Pharm. Sci. 6, 223–228.

Majeed, M.I., Guo, J., Yan, W., Tan, B., 2016. Preparation of magnetic iron oxide nanoparticles (MIONs) with improved saturation magnetization using multifunctional polymer ligand. Polym. (Basel) 8, 1–16. https://doi.org/10.3390/polym8110392.

Cruz, M.S., Rui, Krauter, V., Agriopoulou, S., Weinrich, R., Herbes, C., Scholten, P.B.V., Uysal-unalan, I., Sogut, E., Kopacic, S., Lahti, J., Rutkaite, R., Varzakas, T., 2022. Bioplastics for Food Packaging: Environmental Impact. Trends Regul. Asp., Foods 11, 1–39.

Cartwright, A., Jackson, K., Morgan, C., Anderson, A., Britt, D.W., 2020. A review of metal and metal-oxide nanoparticle coating technologies to inhibit agglomeration and increase bioactivity for agricultural applications. Agronomy 10, 1–20. https://doi.org/10.3390/agronomy10071018.

Castro-Criado, D., Rivera-Flores, O., Abdullah, J.A.A., Castro-Osorto, E., Alonso-González, M., Ramos-Casco, L., Perez-Puyana, V.M., Sánchez-Barahona, M., Sánchez-Cid, P., Jiménez-Rosado, M., Romero, A., 2023. Valorization of Honduran Agro-Food Waste to Produce Bioplastics. Polym. (Basel) 15. https://doi.org/10.3390/polym15122625.

Abdullah, J.A.A., Jiménez-Rosado, M., Perez-Puyana, V., Guerrero, A., Romero, A., 2022. Green Synthesis of FexOy Nanoparticles with Potential Antioxidant Properties. Nanomaterials 12, 2449. https://doi.org/10.3390/nano12142449.

Abdullah, J.A.A., Díaz-García, Á., Law, J.Y., Romero, A., Franco, V., Guerrero, A., 2023a. Sustainable Nanomagnetism: Investigating the Influence of Green Synthesis and pH on Iron Oxide Nanoparticles for Enhanced Biomedical Applications. Polym. (Basel) 15, 3850. https://doi.org/10.3390/polym15183850.

Abdullah, J.A.A., Jiménez-Rosado, M., Guerrero, A., Romero, A., 2023a. Effect of Calcination Temperature and Time on the Synthesis of Iron Oxide Nanoparticles: Green vs. Chemical Method. Mater. (Basel) 16, 1798. https://doi.org/10.3390/ma16051798.

Abdullah, J.A.A., Salah Eddine, L., Abderrhmane, B., Alonso-González, M., Guerrero, A., Romero, A., 2020. Green synthesis and characterization of iron oxide nanoparticles by pheonix dactylifera leaf extract and evaluation of their antioxidant activity. Sustain. Chem. Pharm. 17, 100280 https://doi.org/10.1016/j.scp.2020.100280.

Mohammed, H.A., Eddine, L.S., Souhaila, M., Hasan, G.G., Kir, I., Abdullah, J.A.A., 2023. Green Synthesis of SnO2 Nanoparticles from Laurus nobilis L. Extract for Enhanced Gelatin-Based Films and CEF@SnO2 for Efficient Antibacterial Activity. Food Bioprocess Technol. 1–19. https://doi.org/10.1007/s11947-023-03209-8.

Rajeswari, V.D., Khalifa, A.S., Elfasakhany, A., Badruddin, I.A., Kamangar, S., Brindhadevi, K., 2021. Green and ecofriendly synthesis of cobalt oxide nanoparticles using Phoenix dactylifera L: antimicrobial and photocatalytic activity. Appl. Nanosci. 11 https://doi.org/10.1007/s13204-021-02038-5.

Wang, T., Jin, X., Chen, Z., Megharaj, M., Naidu, R., 2014. Science of the Total Environment Green synthesis of Fe nanoparticles using eucalyptus leaf extracts for treatment of eutrophic wastewater. Sci. Total Environ. 466–467, 210–213. https://doi.org/10.1016/j.scitotenv.2013.07.022.

Chandrasekar, N., Mohan Kumar, K.M., Balasubramnian, K.S., Karunamurthy, K., Varadharajan, R., 2013. Facile synthesis of iron oxide, iron-cobalt and zero valent iron nanoparticles and evaluation of their anti microbial activity, free radicle scavenginging activity and antioxidant assay, Dig. J. Nanomater. Biostructures. 8, 765–775.

Huang, L., Weng, X., Chen, Z., Megharaj, M., Naidu, R., 2014. Synthesis of iron-based nanoparticles using oolong tea extract for the degradation of malachite green. Spectrochim. Acta Part A Mol. Biomol. Spectrosc. 117, 801–804. https://doi.org/10.1016/j.saa.2013.09.054.

Abdullah, N.H., Shameli, K., Abdullah, E.C., Abdullah, L.C., 2017. A facile and green synthetic approach toward fabrication of starch-stabilized magnetite nanoparticles. Chin. Chem. Lett. 28, 1590–1596. https://doi.org/10.1016/j.cclet.2017.02.015.

Salgado, P., Márquez, K., Rubilar, O., Contreras, David, Vidal, G., 2019a. The effect of phenolic compounds on the green synthesis of iron nanoparticles (Fe x O y-NPs) with photocatalytic activity. Appl. Nanosci. 9, 371–385. https://doi.org/10.1007/s13204-018-0931-5.

Guerrero-Pérez, M.O., Patience, G.S., 2020. Experimental methods in chemical engineering: Fourier transform infrared spectroscopy—FTIR. Can. J. Chem. Eng. 98, 25–33. https://doi.org/10.1002/cjce.23664.

Manzo, M., Ahmed, H., Nasrazadani, S., 2020. Study on emission spectral lines of hematite and magnetite for purity's differentiation. AIP Adv. 10 https://doi.org/10.1063/1.5143413.

Tadic, M., Trpkov, D., Kopanja, L., Vojnovic, S., Panjan, M., 2019. Hydrothermal synthesis of hematite (α-Fe2O3) nanoparticle forms: Synthesis conditions, structure, particle shape analysis, cytotoxicity and magnetic properties. J. Alloy. Compd. 792, 599–609. https://doi.org/10.1016/j.jallcom.2019.03.414.

Haavik, C., Stølen, S., Fjellvåg, H., Hanfland, M., Häusermann, D., 2000. Equation of state of magnetite and its high-pressure modification: Thermodynamics of the Fe-O system at high pressure. Am. Mineral. 85, 514–523. https://doi.org/10.2138/am-2000-0413.

Wright, J.P., Bell, A.M.T., Attfield, J.P., 2000. Variable temperature powder neutron diffraction study of the Verwey transition in magnetite Fe3O4. Solid State Sci. 2, 747–753. https://doi.org/10.1016/S1293-2558(00)01107-9.

Wright, J.P., Attfield, J.P., Radaelli, P.G., 2002. Charge ordered structure of magnetite. Phys. Rev. B. 66, 214422 https://doi.org/10.1103/PhysRevB.66.214422.

Abdullah, J.A.A., Díaz-García, Á., Law, J.Y., Romero, A., Franco, V., Guerrero, A., 2023b. Quantifying the Structure and Properties of Nanomagnetic Iron Oxide Particles for Enhanced Functionality through Chemical Synthesis. Nanomaterials 13, 2242. https://doi.org/10.3390/nano13152242.

Vargas, J.M., Lima, E., Socolovsky, L.M., Knobel, M., Zanchet, D., Zysler, R.D., 2007. Annealing effects on 5 nm iron oxide nanoparticles. J. Nanosci. Nanotechnol. 7, 3313–3317. https://doi.org/10.1166/jnn.2007.688.

Demortière, A., Panissod, P., Pichon, B.P., Pourroy, G., Guillon, D., Donnio, B., Bégin-Colin, S., 2011. Size-dependent properties of magnetic iron oxide nanocrystals. Nanoscale. https://doi.org/10.1039/c0nr00521e.

Tuoriniemi, J., Johnsson, A.C.J.H., Holmberg, J.P., Gustafsson, S., Gallego-Urrea, J.A., Olsson, E., Pettersson, J.B.C., Hassellöv, M., 2014. Intermethod comparison of the particle size distributions of colloidal silica nanoparticles. Sci. Technol. Adv. Mater. 15 https://doi.org/10.1088/1468-6996/15/3/035009.

Venkateswarlu, S., Natesh Kumar, B., Prasad, C.H., Venkateswarlu, P., Jyothi, N.V.V., 2014. Bio-inspired green synthesis of Fe3O4 spherical magnetic nanoparticles using Syzygium cumini seed extract. Phys. B Condens. Matter 449, 67–71. https://doi.org/10.1016/j.physb.2014.04.031.

Avolio, M., Gavilán, H., Mazario, E., Brero, F., Arosio, P., Lascialfari, A., Puerto Morales, M., 2019. Elongated magnetic nanoparticles with high-aspect ratio: a nuclear relaxation and specific absorption rate investigation. Phys. Chem. Chem. Phys. 21, 18741–18752. https://doi.org/10.1039/C9CP03441B.

Park, B., Kim, B.H., Yu, T., 2018. Synthesis of spherical and cubic magnetic iron oxide nanocrystals at low temperature in air. J. Colloid Interface Sci. 518, 27–33. https://doi.org/10.1016/j.jcis.2018.02.026.

Islam, M.R., Kamal, M.M., Kabir, M.R., Hasan, M.M., Haque, A.R., Hasan, S.M.K., 2023. Phenolic compounds and antioxidants activity of banana peel extracts: Testing and optimization of enzyme-assisted conditions. Meas. Food 10, 100085. https://doi.org/10.1016/j.meafoo.2023.100085.

Apak, R., Güçlü, K., Demirata, B., Özyürek, M., Çelik, S.E., Bektaşoğlu, B., Berker, K.I., Özyurt, D., 2007. Comparative evaluation of various total antioxidant capacity assays applied to phenolic compounds with the CUPRAC assay. Molecules 12, 1496–1547. https://doi.org/10.3390/12071496.

Kanagasubbulakshmi, S., Kadirvelu, K., 2017. Green synthesis of Iron oxide nanoparticles using Lagenaria siceraria and evaluation of its Antimicrobial activity. Def. Life Sci. J. 2, 422. https://doi.org/10.14429/dlsj.2.12277.

Affes, S., Maalej, H., Aranaz, I., Kchaou, H., Acosta, N., Heras, Á., Nasri, M., Sawsan, A., Maalej, H., Aranaz, I., Kchaou, H., Acosta, N., Heras, Á., Nasri, M., 2020. Controlled size green synthesis of bioactive silver nanoparticles assisted by chitosan and its derivatives and their application in biofilm preparation. Carbohydr. Polym. 236 https://doi.org/10.1016/j.carbpol.2020.116063.

Zhao, X., Zhou, L., Shahid, M., Rajoka, R., Yan, L., Shao, D., Zhu, J., Shi, J., Huang, Q., Yang, H., 2018. Fungal silver nanoparticles: synthesis, application and challenges, Crit. Rev. Biotechnol. Crit. Rev. Biotechnol. 38, 817–835. https://doi.org/10.1080/07388551.2017.1414141.

Rajakumar, G., Thiruvengadam, M., Mydhili, G., Gomathi, T., Chung, I.M., 2018. Green approach for synthesis of zinc oxide nanoparticles from Andrographis paniculata leaf extract and evaluation of their antioxidant, anti-diabetic, and anti-inflammatory activities. Bioprocess Biosyst. Eng. 41, 21–30. https://doi.org/10.1007/s00449-017-1840-9.

Santoyo Salazar, J., Perez, L., De Abril, O., Truong Phuoc, L., Ihiawakrim, D., Vazquez, M., Greneche, J.-M.M., Begin-Colin, S., Pourroy, G., 2011. Magnetic iron oxide nanoparticles in 10–40 nm range: Composition in terms of magnetite/maghemite ratio and effect on the magnetic properties. Chem. Mater. 23, 1379–1386. https://doi.org/10.1021/cm103188a.

Leopoldini, M., Russo, N., Toscano, M., 2011. The molecular basis of working mechanism of natural polyphenolic antioxidants. Food Chem. 125, 288–306. https://doi.org/10.1016/j.foodchem.2010.08.012.

Zeb, A., 2020. Concept, mechanism, and applications of phenolic antioxidants in foods. J. Food Biochem. 44, 1–22. https://doi.org/10.1111/jfbc.13394.

Phenols, H., Rhile, I.J., Markle, T.F., Nagao, H., Dipasquale, A.G., Lam, O.P., a Lockwood, M., Rotter, K., Mayer, J.M., 2006. Concerted Proton - Electron Transfer in the Oxidation of. J. Am. Chem. Soc. 128, 6075–6088 http://pubs.acs.org/doi/abs/10.1021/ja054167+.

Perron, N.R., Wang, H.C., Deguire, S.N., Jenkins, M., Lawson, M., Brumaghim, J.L., 2010. Kinetics of iron oxidation upon polyphenol binding. Dalt. Trans. 39, 9982–9987. https://doi.org/10.1039/c0dt00752h.

Perron, N.R., Brumaghim, J.L., 2009. A review of the antioxidant mechanisms of polyphenol compounds related to iron binding. Cell Biochem. Biophys. 53, 75–100. https://doi.org/10.1007/s12013-009-9043-x.

S. Galus, E. Aytunga, A. Kibar, M. Gniewosz, K. Kra, Novel Materials in the Preparation of Edible Films and Coatings — A Review, (n.d.) 1–14.